National Aviation Academy

International Journal of Transportation Research and Technology

e-ISSN: 3079-6075

DOI: 10.71108/transporttech.vm02is02.04

Research Article

Comparative Evaluation of PID and Fuzzy Electronic Stability Control via Differential Braking in a Double Lane Change Maneuver

Dinh-Dung Nguyen*[1], Ngoc-Tuan Vu[1], Danh-Dong Tran[2], Manh-Hung Duong[1]

[1]*Le Quy Don Technical University, Hanoi, Vietnam*

[2]*Engineering Technology College of the Central Vietnam, Khanh Hoa, Vietnam*

Timescale of article

Received: 30 October 2025
Accepted: 11 November 2025
Published: 25 December 2025

Corresponding author

Dinh-Dung Nguyen
dungnd@lqdtu.edu.vn

Keywords

Electronic Stability Control, Differential braking, Yaw stability, PID controller, Fuzzy Logic Controller

Cite this article as:

Nguyen, D.-D., Vu, N.-T., Tran, D.-D. & Duong, M.-H. (2025). Comparative Evaluation of PID and Fuzzy Electronic Stability Control via Differential Braking in a Double Lane Change Maneuver. *International Journal of Transportation Research and Technology*, 2(2), 55-65. DOI: 10.71108/transporttech.vm02is02.04

Abstract

Electronic Stability Control (ESC) is central to preventing loss-of-control crashes, yet its on-road behavior still reflects design trade-offs between rapid error correction and ride comfort. This study builds a high-fidelity ESC evaluation platform by coupling a spatial vibration model with a two-track handling model in a CarSim–MATLAB/Simulink co-simulation. Two representative controllers—a classical PID and a fuzzy-logic design—utilize identical inputs (driver steering angle and measured yaw rate) and a common supervisory layer (a dead-zone around minor errors and left/right brake distribution logic). Interventions are applied as wheel-specific brake pressures; the fuzzy controller employs nine membership sets for yaw rate and steering and five for brake pressure. Performance is assessed in an ISO-style Double Lane Change at 40 km/h using trajectory RRMSE, yaw-rate IAE, control-effort IACA (from brake pressure), and peak lateral acceleration.

Both controllers keep the vehicle close to the reference path (RRMSE < 10%). The PID achieves faster yaw-rate convergence and smaller IAE but at the cost of higher control activity (larger IACA) and more pronounced oscillations, particularly in lateral acceleration. The fuzzy controller yields smoother, step-like brake actions that reduce oscillatory behavior and control effort, while converging more slowly. These head-to-head results quantify a practical trade-off relevant to calibration: prioritize PID when rapid stabilization is paramount, or favor fuzzy logic when comfort and restraint of intervention are critical. The framework provides a reproducible basis for ESC benchmarking and suggests targeted tuning of PID gains and fuzzy rule bases, as well as extensions to advanced controllers (e.g., LQR, MPC), for improved stability and comfort balance.

1. Introduction

Electronic Stability Control (ESC) is a mature technology that prevents loss of control by generating corrective yaw moments-typically via differential braking or individual wheel torque control. In the recent literature, three complementary trends stand out. First, there is continued interest in classical designs because of their transparency and ease of calibration, including PID-based yaw-rate tracking tailored for ESC (Arronte et al., 2023). Second, researchers strive for real-time, implementable solutions that directly act on wheel torques/pressures while estimating or regulating both yaw rate and sideslip (Tristano et al., 2022). Third, more advanced or hybrid formulations aim to balance yaw-rate and sideslip objectives under varying tire–road conditions (Gimondi et al., 2021), or to explicitly cope with delays and uncertainties introduced by sensing, computation, and brake actuators (Wang et al., 2022). These developments are accompanied by broader surveys that contextualize stability control for electrified powertrains and brake-by-wire architectures (Anand & Srinivaas, 2023) and by adaptive schemes oriented toward electric-braking implementations in production-like settings (Hieu, 2024). General overviews of ESC fundamentals remain relevant for framing system objectives and evaluation procedures (Gupta et al., 2020).

Despite this progress, several practical challenges persist. Vehicle lateral dynamics are nonlinear and strongly dependent on tire–road friction, speed, and steering inputs; a controller tuned for one regime may over- or under-actuate in another. Aggressive tracking can quickly reduce yaw-rate error, but may excite oscillations in lateral acceleration and degrade ride comfort; gentler or quantized actions improve comfort but risk slower convergence. Realistic execution involves non-negligible sensing/communication delays, as well as actuator limits/saturation (Wang et al., 2022), and modern ESCs must allocate left/right brake pressure (or wheel torque) to synthesize the desired yaw moment without chattering. Finally, credible assessment requires representative testbeds-e.g., two-track (double-track) vehicle models and standardized maneuvers such as the Double Lane Change (DLC)—and metrics that expose tracking–effort–comfort trade-offs.

Motivated by these gaps, this study builds a co-simulation testbed (CarSim for high-fidelity vehicle dynamics; MATLAB/Simulink for reference generation and control logic) and implements two philosophically different ESC strategies under identical conditions: a PID controller and a fuzzy-logic controller (a common heuristic approach in ESC practice). The vehicle executes an ISO-style DLC at 40 km/h, and performance is evaluated using (i) trajectory-tracking error (e.g., RRMSE), (ii) yaw-rate tracking error (IAE), (iii) control activity based on brake pressure (IACA), and (iv) peak lateral acceleration.

Building on the system descriptions translated earlier, the paper's main contributions are:

- Integrated modeling and execution: a coupled spatial-plus–two-track vehicle model in a CarSim–Simulink co-simulation loop that produces sensor-level signals and wheel-level brake commands suitable for ESC studies.
- Fair, head-to-head comparison: PID (continuous action) and fuzzy logic (step-like action) are embedded in the same supervisory structure (dead-zone around minor errors and left/right brake-distribution logic tied to yaw-rate error sign), enabling an apples-to-apples evaluation.
- Quantitative trade-off evidence: results on RRMSE/IAE/IACA and lateral-acceleration peaks show that PID achieves faster yaw-rate regulation with higher control activity and greater oscillation risk, whereas fuzzy logic yields smoother behavior with lower intervention but slower convergence-findings that align with recent practice-oriented ESC studies.
- Actionable guidance for tuning and extensions: the study identifies areas where PID gains and fuzzy rule bases warrant optimization, pointing to future exploration of adaptive/advanced schemes suited to electric-brake systems and delay-aware designs.

Together, these results provide a concise, evidence-based understanding of how PID and fuzzy controllers behave in an ESC context, offering a reproducible path to extend the analysis to alternative control laws, vehicle platforms, and road conditions.

2. Method

2.1. Vehicle dynamics model

The vehicle dynamics framework comprises 14 degrees of freedom, organized into two submodels: a seven-degree-of-freedom (DOF) spatial (ride) vibration model and a seven-DOF planar (handling) model. These DOFs include six rigid-body motions of the vehicle-translation and rotation about the x, y, and z axes-plus four vertical motions for the suspension units and four wheel-spin states. In the spatial vibration model (Fig. 1), the body is treated as perfectly rigid; springs and dampers are modeled as linear elements; tire resistance is neglected; and the road is assumed to be flat and uniform.

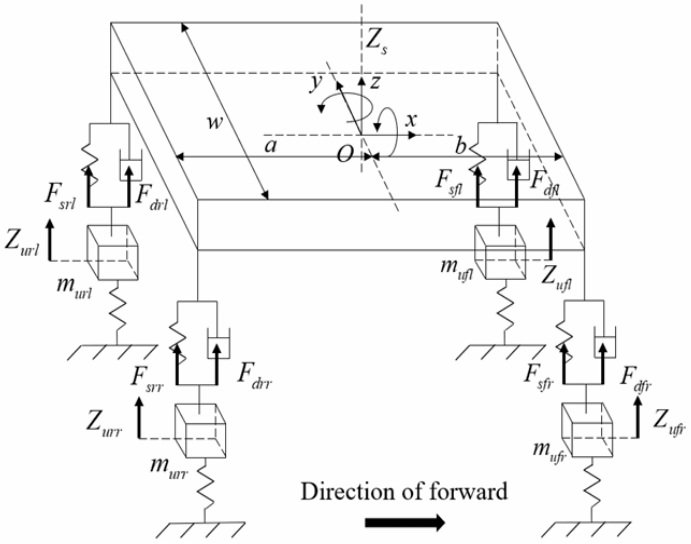

Fig. 1. Dynamic model of Vehicle (Wu et al., 2024)

Fig. 2 presents a double-track (two-track) vehicle model for analyzing the car's motion under these assumptions: elastic tires roll on a rigid roadway and remain in continuous contact; all wheels share the same constant rolling-resistance coefficient; aerodynamic drag and the static load are symmetrically distributed about the vehicle's direction of travel; steering is applied at the front axle with identical steering angles on the two front wheels. The coordinate axes are oriented as shown in the figure. For rotational variables, the positive sense is defined as counterclockwise when viewed from above.

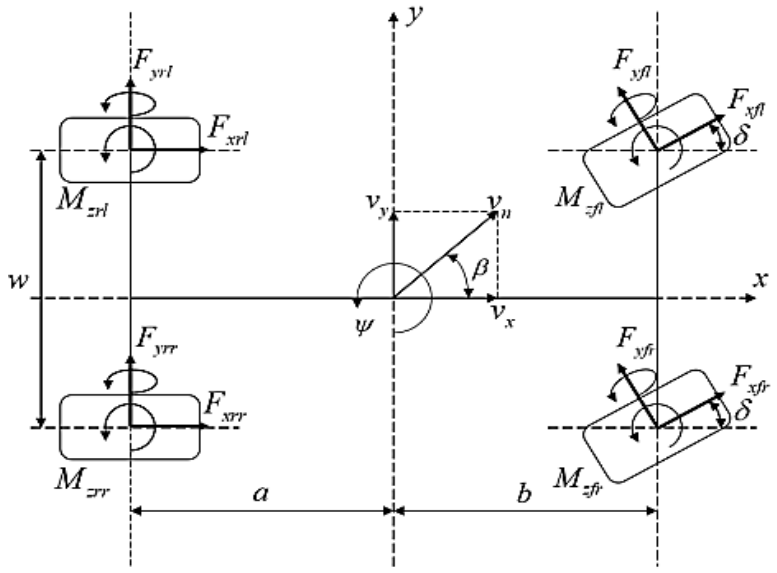

Fig. 2. Dynamic model of two-track motion of a Vehicle (Wu et al., 2024)

Dynamic equations of a Vehicle (Wu et al., 2024)

$$F_{xfl}\cos\delta - F_{yfl}\sin\delta + F_{xfr}\cos\delta - F_{yfr}\sin\delta + F_{xrl} + F_{xrr} = m_t(\dot{v}_x - v_y\dot{\psi}) \quad (1)$$

$$F_{yfl}\cos\delta + F_{xfl}\sin\delta + F_{yfr}\cos\delta + F_{xfr}\sin\delta + F_{yrl} + F_{yrr} = m_t(\dot{v}_y + v_x\dot{\psi}) \quad (2)$$

$$\frac{w}{2}F_{xfl}\cos\delta + \frac{w}{2}F_{xfr}\cos\delta - \frac{w}{2}F_{xrl} + \frac{w}{2}F_{xrr} + \frac{w}{2}F_{yfl}\sin\delta - \frac{w}{2}F_{yfr}\sin\delta + bF_{xfl}\sin\delta + bF_{yfl}\cos\delta + bF_{xfr}\sin\delta + bF_{yfr}\cos\delta - aF_{yrl} - aF_{yrr} + M_{zfl} + M_{zfr} + M_{zrl} + M_{zrr} = I_z\ddot{\psi} \quad (3)$$

Where, F_{sfl}, F_{sfr}, F_{srl}, F_{srr} - elastic force of suspension at left front wheel, right front wheel, left rear wheel and right rear wheel;

F_{dfl}, F_{dfr}, F_{drl}, F_{drr} - suspension damping resistance at the front left wheel, front right wheel, rear left wheel and rear right wheel;

a, b - the distances from the center of gravity to the rear and front axles;

w - the wheelbase of the vehicle;

I_x, I_y - moment of inertia of suspended mass about x-axis and y-axis;

F_{xfl}, F_{xfr}, F_{xrl}, F_{xrr} - force acting in x direction at left front wheel, right front wheel, left rear wheel and right rear wheel;

F_{yfl}, F_{yfr}, F_{yrl}, F_{yrr} - force acting in y direction at left front wheel, right front wheel, left rear wheel and right rear wheel;

m_t - the mass of the vehicle; δ - the steering angle;

F_{tfl}, F_{tfr}, F_{trl}, F_{trr} - elastic force of tire at left front wheel, right front wheel, left rear wheel and right rear wheel;

m_{ufl}, m_{ufr}, m_{url}, m_{urr} - the mass must not be suspended from the front left wheel, front right wheel, rear left wheel and rear right wheel;

Z_{ufl}, Z_{ufr}, Z_{url}, Z_{urr} - displacement of unsprung mass at left front wheel, right front wheel, left rear wheel and right rear wheel;

M_{zfl}, M_{zfr}, M_{zrl}, M_{zrr} - moment around z-axis at left front wheel, right front wheel, left rear wheel and right rear wheel;

The system of equations representing the dynamics of four wheels is as follows:

$$I_w\dot{\omega}_{fl} = M_{dfl} - M_{bfl} - F_{xfl}R_w \quad (4)$$

$$I_w\dot{\omega}_{fr} = M_{dfr} - M_{bfr} - F_{xfr}R_w \quad (5)$$

$$I_w\dot{\omega}_{rl} = M_{drl} - M_{brl} - F_{xrl}R_w \quad (6)$$

$$I_w\dot{\omega}_{rr} = M_{drr} - M_{brr} - F_{xrr}R_w \quad (7)$$

Where, I_w, R_w - moment of inertia and dynamic radius of the wheels;

ω_{fl}, ω_{fr}, ω_{rl}, ω_{rr}; M_{dfl}, M_{dfr}, M_{drl}, M_{drr}; M_{bfl}, M_{bfr}, M_{brl} , M_{brr} - angular velocity, transmitted driving torque and braking torque at the front left wheel, front right wheel, rear left wheel and rear right wheel.

2.2. PID controller synthesis

The PID controller is formulated to minimize the tracking error eee between the target body angular velocity (e.g., yaw rate) and the measured body angular velocity during vehicle operation.

The actual body angular velocity is obtained from the sensor signal (fed by the CarSim vehicle-dynamics simulation block), while the desired body angular velocity is computed from the steering angle and vehicle speed (via the MATLAB/Simulink calculation block) using the following equation:

$$"\psi" \ "=" \ ("\delta" "x" \ )/("a+b+" \ ("m" ("x ") "(a" "C" \_"\alpha r" \ "- b" "C" \_"\alpha f" \ ")")/("2" "C" \_"\alpha r" \ "C" \_"\alpha f" \ )) \quad (8)$$

Where, "C" _"αr" , "C" _"αf" - lateral stiffness of front and rear tires

Fig. 3 illustrates an Electronic Stability Control (ESC) scheme governed by a PID controller. The main elements include the inputs-vehicle speed, steering angle, and measured yaw rate-together with a block that computes the reference (desired) yaw rate and the PID controller itself. A Dead Zone block follows the PID to introduce a small deadband, filtering out minor errors (noise or tiny offsets) so the ESC doesn't intervene unnecessarily. The Product (×) block scales the PID output by a brake-distribution vector, and a downstream Switch selects among three control commands corresponding to different instability scenarios. The switch uses the post–Dead Zone signal as its condition: a positive value biases braking to the left to create a counter-clockwise yaw moment (viewed from above), while a negative value biases braking to the right to generate a clockwise yaw moment.

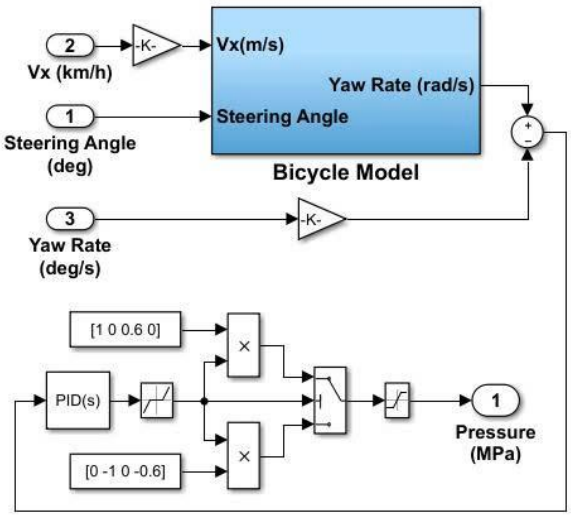

Fig. 3. The Electronic stability control system with a PID controller (Source: Authors' own work)

When the switch input is zero, it selects a zero command, meaning no control action is applied. The PID controller takes the tracking error between the desired and measured body angular velocity (yaw rate) as input and provides a brake-pressure command for each wheel.

The method of synthesizing the parameters of the PID controller is presented in (Nguyen et al., 2025). Applying this method, the parameters of the PID controller are synthesized as follows:

$$KP = 37; KI = 100; KD = 0.1.$$

2.3. Fuzzy logic controller design

The study designs the fuzzy controller using MATLAB® (Natick, MA, USA) and the Fuzzy Logic Toolbox™. As a first step, the input and output variables are specified. For the ESC, the inputs are the vehicle's yaw rate and the driver's steering angle (see Fig. 4). The ESC becomes active when the brake pedal is applied and deactivates once the vehicle speed falls below 8 km/h. Its output is the commanded brake pressure, which is fed to the CarSim vehicle-dynamics model. The ESC's fuzzy controller issues commands for both sides of the vehicle, allowing the system to increase brake pressure on either the right or left wheels, depending on the sign of the body's rotational motion.

Both the inputs and the output are modeled using fuzzy membership sets Hi (for i = 1, 2,...). The first input to the fuzzy controller is the vehicle's yaw rate, partitioned into nine fuzzy sets H1–H9 over a universe of discourse from [−4, 4] (Fig. 4(a)). The second input is the steering angle, which likewise employs nine symmetrically arranged sets over [−180 o, 180 o] (Fig. 4(b)). We assume that, in emergency conditions, the driver's steering action is limited to a half-turn of the wheel to either side—an overall range of 360 o. The braking system's maximum pressure in this

study is 6.5 MPa. The output variable, brake pressure p (Fig. 4(c)), spans the range [0, 6.5] MPa and is described by five membership sets, H1–H5.

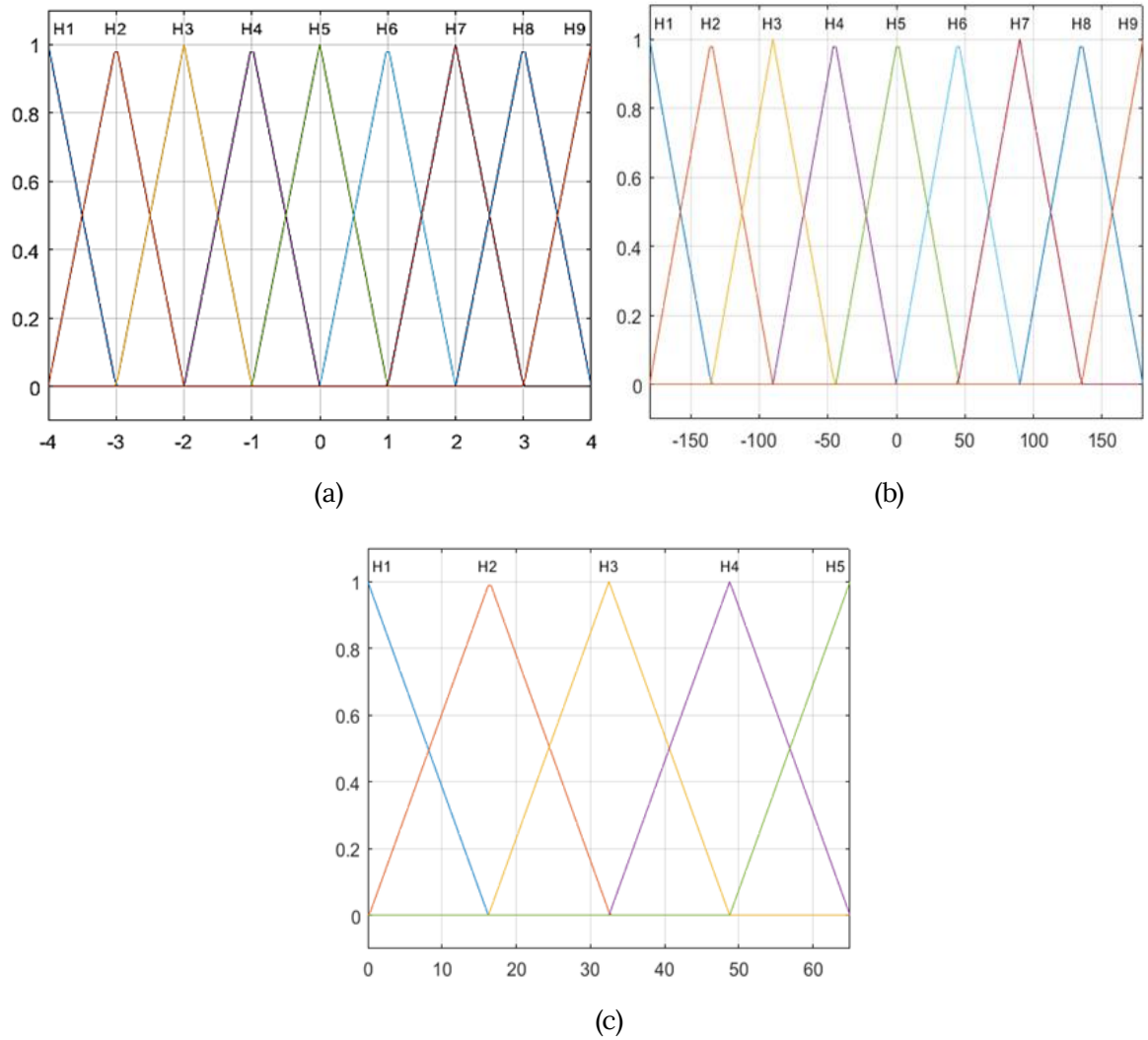

Fig. 4. Input and output of fuzzy logic controller: (a) Input ψ; (b) Input δ; (c) Output p. (Source: Authors' own work)

Fig. 5 illustrates the electronic stability control system with a Fuzzy-Logic Controller. The steering angle (deg) and measured yaw rate (deg/s) are fed into the fuzzy-logic block, which outputs a normalized brake demand. This demand is split into left and right channels and weighted by distribution gains to set wheel-brake pressures. Positive output biases the left side and negative the right, producing a corrective yaw moment; the combined signal yields the commanded brake pressure (MPa).

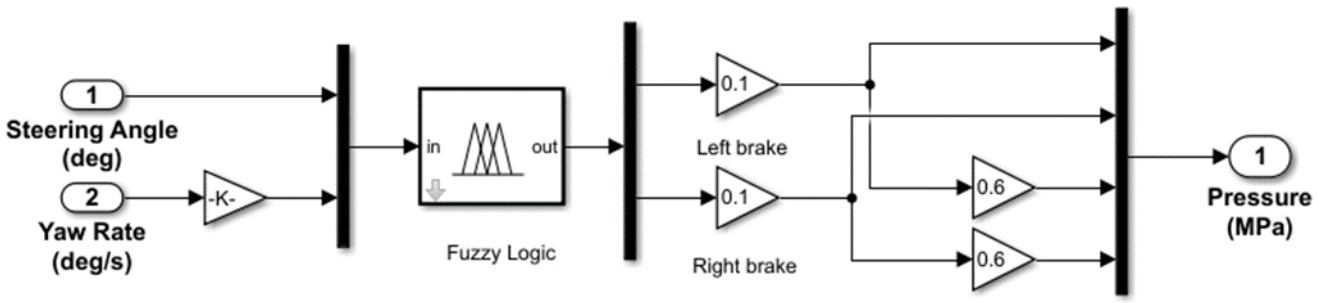

Fig. 5. The Electronic stability control system with a Fuzzy Logic controller (Source: Authors' own work)

3. Results and Discussion

The ESC is evaluated in CarSim using a D-Class SUV. The CarSim vehicle parameters were provided in the Appendix 1. The test maneuver is a double-lane change (Fig. 6) performed at a constant 40 km/h.

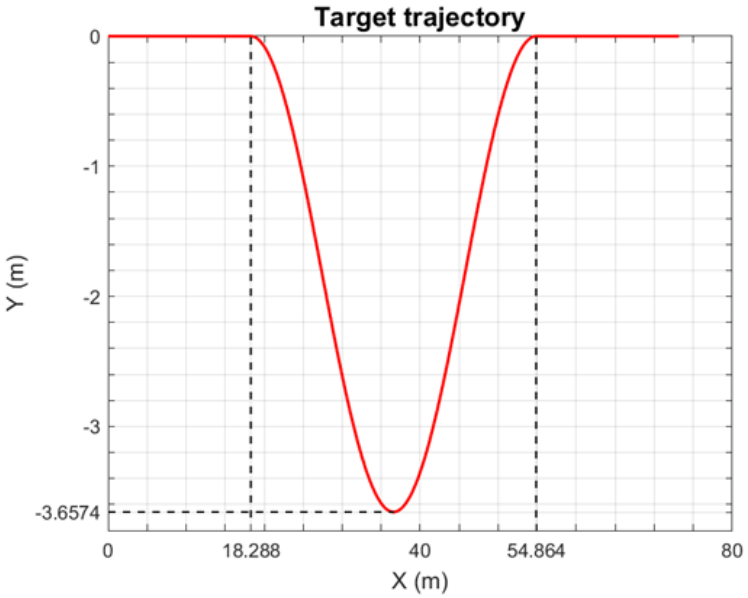

Fig. 6. Dual lane change simulation trajectory (Source: Authors' own work)

Fig. 7 plots the vehicle's center-of-mass path in the double-lane-change test under both PID and fuzzy-logic control. In each case, the trajectory of the vehicle's center of gravity stays close to the desired path, and the vehicle settles stably as it returns to the correct lane.

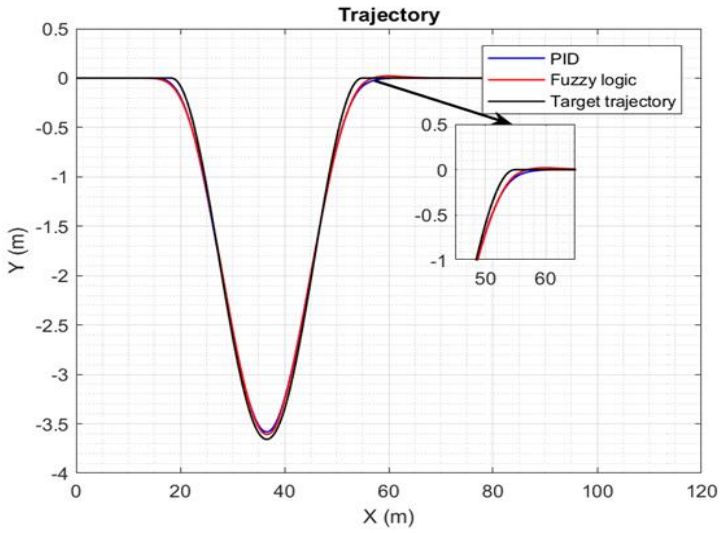

Fig. 7. Trajectory of the vehicle's center of gravity with PID controller and Fuzzy Logic (Source: Authors' own work)

Fig. 8 presents the time histories of steering angle (Fig. 8(a)), lateral acceleration (Fig. 8(b)), vehicle yaw rate (Fig. 8(c)), and yaw-rate tracking error (Fig. 8(d)). When comparing the two controllers, it is clear that the PID controller suppresses the yaw-rate error (Fig. 8(d)) more effectively, bringing the yaw rate (Fig. 8(c)) to its target faster than the fuzzy-logic scheme. However, this improvement comes at a cost: the PID controller produces larger oscillations-especially in lateral acceleration (Fig. 8(b))-which can cause noticeable shake or discomfort for vehicle occupants during the lane-change maneuver.

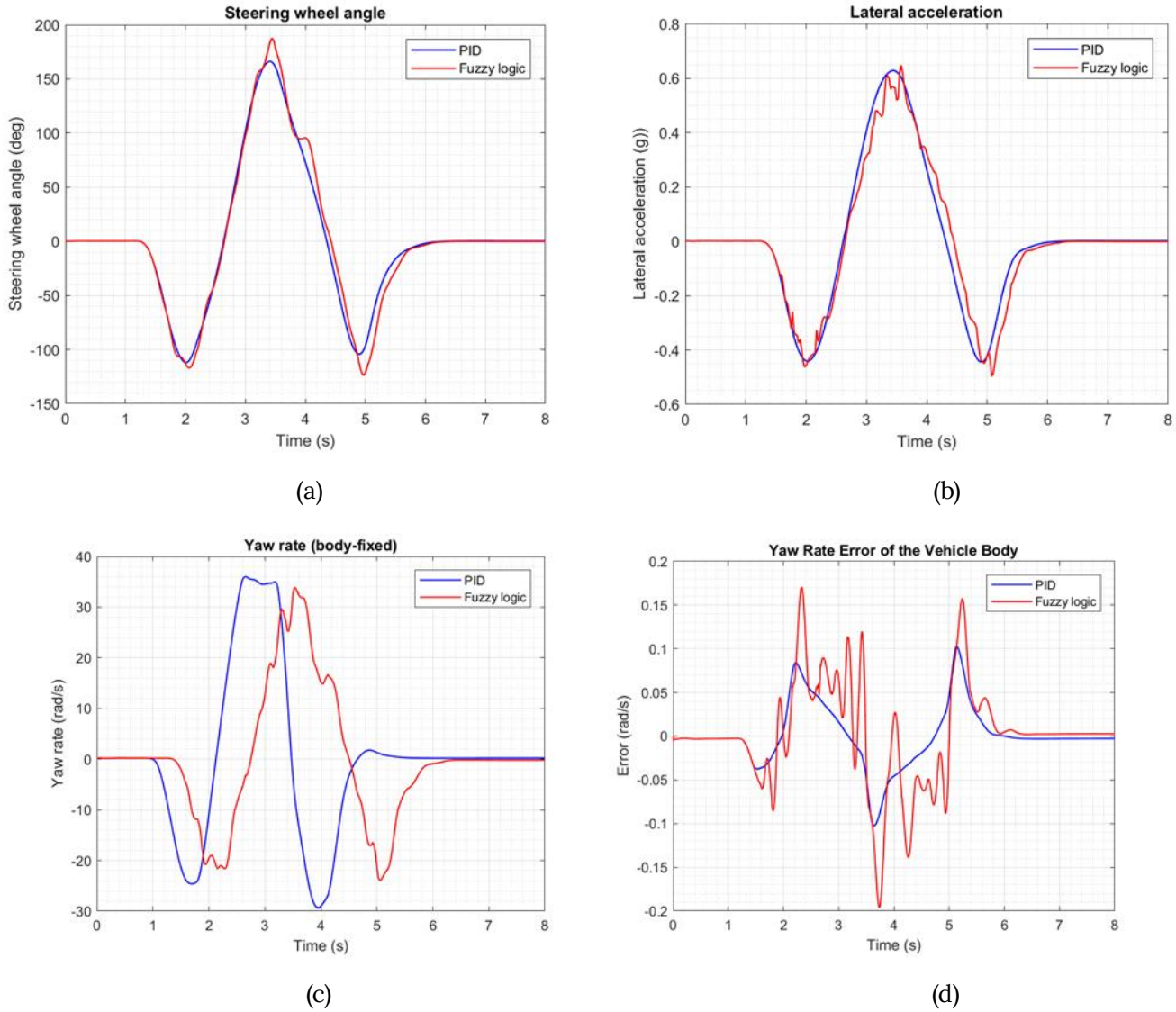

Fig. 8. Simulation results of ESC system with PID controller and Fuzzy logic: (a) Steering angle; (b) Lateral acceleration; (c) Vehicle body angular velocity; (d) Vehicle body angular velocity deviation (Source: Authors' own work)

Fig. 9 shows wheel-brake pressures under PID (Fig. 9(a)) and fuzzy-logic (Fig. 9(b)) controllers. Modulating individual wheel pressure is crucial for balance and stability. If the vehicle tends toward oversteer or understeer, the ESC adjusts pressure at select wheels to generate a corrective yaw moment, guiding the yaw rate toward its reference. This intervention appears as time-varying pressure traces for each wheel in Fig. 9a and 9b.

With the PID controller, brake pressure changes continuously (smooth curves), enabling a rapid response to yaw-rate error but also tending to excite oscillations that can reduce stability—most notably in lateral dynamics. The fuzzy controller, by contrast, issues step-like (quantized) pressure commands that make the braking action more settled and suppress unwanted oscillations, though the response can be slower in some urgent scenarios. Consequently, PID is preferable when fast reaction is the priority.

To compare the two controllers quantitatively, we report the following metrics: the mean-squared relative trajectory error, the integral of absolute error (IAE), the integral of absolute control activity based on brake pressure (IACA), and the peak lateral acceleration. The IAE and IACA values, in particular, indicate the tracking performance and the control effort required by each strategy.

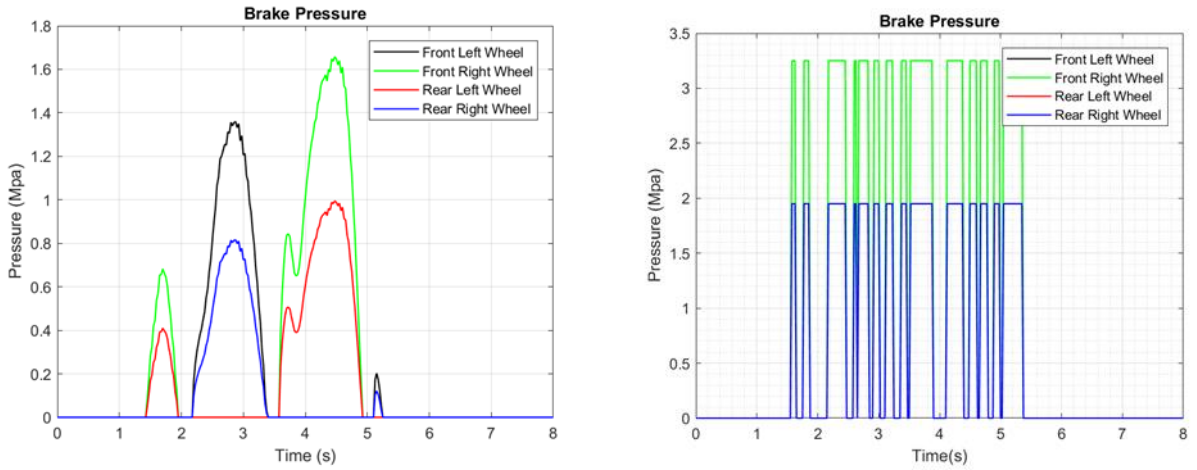

(a) (b)

Fig. 9. Brake pressure on wheels with PID controller (a) and Fuzzy Logic (b). (Source: Authors' own work)

Table 1 shows the comparison of results when simulating the ESC system with PID and Fuzzy Logic controllers.

Table 1. Comparison of results when simulating the ESC system with PID and Fuzzy Logic controllers

	Trajectory	**Vehicle body angular velocity deviation**	**Maximum horizontal acceleration**	**Brake pressure**
	RRMSE	**IAE**	**a_{max}**	**IACA**
PID controller	0.21%	0.177	0.797	100.40
Fuzzy Logic controller	0.49%	0.304	0.648	120.44

From Table 1, the fuzzy-logic controller intervenes less—indicated by a lower IACA (larger IACA implies greater cumulative intervention (higher control effort))—and therefore shows a larger yaw-rate tracking error, as seen in the higher IAE. This is partly attributable to a rule base that has not been fully optimized. By comparison, the PID controller keeps the yaw-rate error more minor but requires more frequent/stronger actuation.

As a result, the PID case yields a trajectory that follows the reference more closely (lower RRMSE). Even so, both controllers maintain acceptable path adherence relative to the designed trajectory, with RRMSE values of less than 10% in both scenarios.

Why 40 km/h DLC remains non-trivial. The ISO 3888 double-lane-change imposes tight lateral displacement over a short longitudinal distance. Even at 40 km/h, the required curvature produces peak lateral acceleration nearing the tire linearity limit for compact vehicles on dry asphalt. Transient effects—tire relaxation length, yaw inertia, and coupling between longitudinal deceleration from differential braking and front-axle cornering—induce overshoot/undershoot in yaw rate and sideslip. Because ESC authority is realized via brake torque, interventions reduce speed and can shift the vehicle toward understeer during high-demand segments, complicating precise path following.

Expected changes at higher speeds. Small increases in speed materially raise required tire slip angles and the likelihood of local saturation. We therefore expect (i) larger yaw-rate overshoot and longer settling, (ii) higher IACA (more intervention) for both controllers, and (iii) a sharper trade-off between tracking accuracy and comfort (jerk). Controllers that emphasize damping (e.g., fuzzy) should maintain smoother lateral acceleration but will likely require more anticipatory logic or gain/rule scheduling with speed to preserve path accuracy. We have flagged a speed-sweep study (e.g., 40–80 km/h) as future work to quantify these trends.

4. Conclusions

This study develops a vehicle dynamics framework that couples a spatial ride model with a two-track handling model, utilizing a CarSim–Simulink co-simulation setup. On this basis, two ESC strategies—one PID-based and one fuzzy-logic—are designed to modulate brake pressure at individual wheels, aiming to stabilize the vehicle

during a 40 km/h double-lane change test. The simulations show that both controllers keep the vehicle on the intended path and maintain stable behavior.

The PID approach achieves tighter yaw-rate tracking by issuing continuously varying brake commands, while the fuzzy controller intervenes more conservatively yet still preserves satisfactory path following. This comparison clarifies the trade-offs and supports the selection of suitable control laws for practical ESC deployment. Both methods are viable, but performance depends on tuning—PID gains and fuzzy linguistic rules should be further optimized. Future directions include systematic gain optimization, refining the fuzzy rule base for the ESC, and assessing alternative or hybrid schemes, such as the Linear Quadratic Regulator (LQR) and Model Predictive Control (MPC), to further improve stability and accuracy.

Abbreviations

ESC : Electronic Stability Control

LQR : Linear Quadratic Regulator

MPC : Model Predictive Control

PID : Proportional-Integral-Derivative

References

Anand, L., & Srinivaas, A. (2023). A Review Paper of Electric Vehicle Stability Control. *2023 3rd International Conference on Electrical, Computer, Communications and Mechatronics Engineering* (ICECCME), 1–10. https://doi.org/10.1109/ICECCME57830.2023.10253088

Arronte, C. A., Ripari, G. A., Angélico, B. A., & Colón, D. (2023). Design and Validation of PID Controller for Electronic Stability Control. *2023 15th IEEE International Conference on Industry Applications* (INDUSCON), 343–350. https://doi.org/10.1109/INDUSCON58041.2023.10374967

Gimondi, A., Corno, M., & Savaresi, S. M. (2021). A Mixed Sideslip Yaw Rate Stability Controller for Over-Actuated Vehicles. *ASME 2021 International Design Engineering Technical Conferences and Computers and Information in Engineering Conference*, DETC 2021-68260, V001T01A001. https://doi.org/10.1115/DETC2021-68260

Gupta, S., Hiremath, N., Raut, S., Datkhile, G., & Trivedi, P. (2020). Electronic Stability Control of Vehicles. *ITM Web Conference*, 32, 01009. https://doi.org/10.1051/itmconf/20203201009

Hieu, L. D. (2024). Design of adaptive controller to improve stability for electric vehicles. *The University of Danang - Journal of Science and Technology*, 22(12), 36–43. https://doi.org/10.31130/ud-jst.2024.336

Nguyen, D.-D., Duong, M.-H., & Hoang, Q.-C. (2025). Enhancing altitude control in quadrotors: a study on PID parameter selection and Euler angle influence. *International Journal of Sustainable Aviation*, 11(3), 251–270. https://doi.org/10.1504/IJSA.2025.148747

Tristano, M., Lenzo, B., Xu, X., Forrier, B., D'Hondt, T., Risaliti, E., & Wilhelm, E. (2022). Real-time implementation of yaw rate and sideslip control through individual wheel torques. *2022 IEEE Vehicle Power and Propulsion Conference* (VPPC), 1–6. https://doi.org/10.1109/VPPC55846.2022.10003363

Wang, S., Fan, Z., Li, B., Tang, X., Chen, Z., Zhou, Q., & Wu, J. (2022). Research on adaptive control of input time delay for vehicle electronic stability control system. *2022 6th CAA International Conference on Vehicular Control and Intelligence* (CVCI), 1–5. https://doi.org/10.1109/CVCI56766.2022.9965053

Wu, Z., Kang, C., Li, B., Ruan, J., & Zheng, X. (2024). Dynamic Modeling, Simulation, and Optimization of Vehicle Electronic Stability Program Algorithm Based on Back Propagation Neural Network and PID Algorithm. *Actuators*, 13(3), 100. https://doi.org/10.3390/act13030100

Appendix 1.

Table A1

Parameters	Value
Mass of Vehicle	1429 kg
Moments of inertia	I_x = 1765 kg.m^2; I_y = 377 kg.m^2; I_z = 1765 kg.m^2
Brake torque/brake pressure ratio	Front wheel: 350 Nm/Mpa; Rear wheel: 200 Nm/Mpa
Length, width, height	4.8 m; 1.8 m; 1.7 m
Engine power	150 kW